Effect of Flexible Spacer Length on the Phase Transitions and Mesophase Structures of Main-Chain Thermotropic Liquid-Crystalline Polyesters Having Bulky Pendent Side Groups[†]

Sukky Chang and Chang Dae Han*

Department of Polymer Engineering, The University of Akron, Akron, Ohio 44325-0301

Received November 26, 1996; Revised Manuscript Received January 15, 1997[⊗]

ABSTRACT: The effect of flexible spacer length on the phase transitions and mesophase structures of main-chain thermotropic liquid-crystalline polyesters having bulky pendent side groups was investigated using differential scanning calorimetry (DSC), wide-angle X-ray diffraction (WAXD), and polarizing optical microscopy (POM). For the investigation, a homologous series of poly[(phenylsulfonyl)-*p*-phenylene alkylenebis(4-oxybenzoate)]s (PSHQ*n*) having varying lengths (*n*) of methylene groups of flexible spacers ($n = 3-12$) were synthesized in our laboratory. Using POM we observed that all PSHQ*n* synthesized, with the exception of PSHQ3, have only a schlieren-textured nematic mesophase at temperatures between a glass transition temperature (or melting point) and the isotropization temperature; the nematic−isotropic transition temperature exhibits odd−even fluctuation with the number of methylene groups of the flexible spacer. We found that the isotropization enthalpy and isotropization entropy for PSHQ*n* do not follow a linear relationship with the number of methylene groups when the flexible spacer length becomes shorter than 7, which deviates from the findings for linear main-chain TLCPs reported in the literature. We ascribe this difference to the presence of bulky pendent arylsulfonyl side groups in the main-chain of PSHQ*n*. We found from both DSC and WAXD that (i) PSHQ*n* having odd numbers (5−11) of methylene groups exhibit a glassy nematic mesophase, while PSHQ3, having three methylene groups, has no liquid crystallinity, becoming an amorphous polymer with a glass transition temperature of 129 °C, and (ii) among the PSHQ*n* having even numbers (4−12) of methylene groups, PSHQ4 showed the highest degree of ordering in the crystalline structure. WAXD of PSHQ*n* melt-drawn fibers showed an odd−even fluctuation of chemical repeat unit *d*-spacing, very similar to that reported in the literature for linear main-chain TLCPs.

1. Introduction

In the past, a number of investigators[1−13] reported on the synthesis of main-chain thermotropic liquid-crystalline polymers (TLCPs) with varying spacer lengths and discussed odd−even fluctuation transition temperatures. Using differential scanning calorimetry (DSC), polarizing optical microscopy (POM), and/or wide-angle X-ray diffraction (WAXD), they found that TLCPs having even numbers of methylene groups of flexible spacer have higher clearing temperature than TLCPs having odd numbers of methylene groups. Flexible spacers have been introduced to main-chain TLCPs with rigid backbones in order to lower their melting and clearing temperatures. Such efforts were motivated by the desire to make very rigid rodlike TLCPs processable at a reasonable range of temperatures without thermal degradation. The introduction of flexible spacers alone was found to have little effect on lowering clearing temperatures of TLCPs and thus attempts, with some success, were made to attach either substituents or bulky pendent side groups to the main chain, in order to further lower melting and clearing temperatures.[14−16] The readers are referred to review articles for details.[17−19] Also, a number of investigators[8,9,11,13,20−24] reported on the effect of flexible spacers on the mesophase structures of linear TLCPs.

Recently, we synthesized a homologous series of polyesters, poly[(phenylsulfonyl)-*p*-phenylene alkylenebis(4-oxybenzoate)]s (PSHQ*n*), with chemical structure

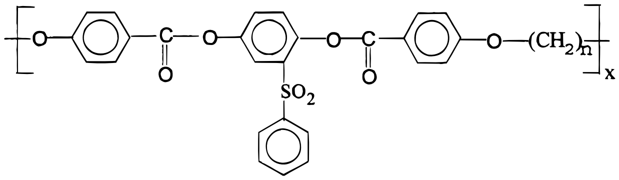

having odd numbers (n = 3, 5, 7, 9, or 11) or even numbers (n = 4, 6, 8, 10, or 12) of methylene groups of flexible spacer and bulky pendent arylsulfonyl side groups, and investigated their mesophase structures using DSC, WAXD, and POM. We have observed some unusual results which deserve the attention of polymer scientists. In this paper, we present the highlights of our findings, putting emphasis on the odd−even effect of flexible spacers on the mesophase structures of the PSHQ*n* synthesized.

2. Experimental Section

PSHQ*n* with *n* ranging from 3 to 12 were synthesized via solution polymerization in dichloromethane, using the procedure described elsewhere.[15,25] Intrinsic viscosities ($[\eta]$) were measured and the results are summarized in Table 1.

For DSC and WAXD measurements, specimens of PSHQ*n* (n = 5, 7−12) with a thickness of 0.5 mm were prepared by solvent casting from dichloromethane in the presence of an antioxidant (Irganox 1010, Ciba-Geigy Group) and then slowly evaporating the majority of the solvent first at room temperature for one week and then at $T_g - 10$ °C for 3 days in a vacuum oven to remove any residual solvent. Specimens of PSHQ4 and PSHQ6 were cast from 1,1,2,2-tetrachloroethane because they did not dissolve in dichloromethane. Sample preparation procedures employed for WAXD of melt-drawn fibers are described elsewhere.[26] For taking micrographs using POM, specimens were prepared by casting from a 1 wt %

[†] This paper is dedicated to Professor Robert W. Lenz, who first reported (ref 15) on the synthesis of the polymers investigated in this study.

[⊗] Abstract published in *Advance ACS Abstracts,* February 15, 1997.

S0024-9297(96)01730-5 CCC: $14.00

Table 1. Summary of the Intrinsic Viscosities and Transition Temperatures of PSHQ*n* Synthesized in This Study

polymer	[η] (dL/g) at 23 °C	T_g (°C)	T_{NI} (°C)
PSHQ3	0.488	129.1	
PSHQ4	0.760	128.2	259.2
PSHQ5	0.547	104.1	167.7
PSHQ6	0.877	109.9	228.0
PSHQ7	0.867	92.1	171.4
PSHQ8	0.666	101.1	198.5
PSHQ9	0.823	84.4	162.1
PSHQ10	0.667	91.8	181.1
PSHQ11	0.485	77.1	147.0
PSHQ12	1.003	84.6	166.9

solution of 1,1,2,2-tetrachloroethane on a slide glass to make a thin film of about 2−3 μm in thickness.

Thermal transition temperatures of all specimens were determined by using a differential scanning calorimeter (du Pont 9900), under a nitrogen atmosphere, at heating and/or cooling rates of 20 °C/min. The thermal histories (namely, annealing temperature and the duration of annealing) of the specimens were varied.

WAXD experiments were conducted at room temperature on both melt-drawn fibers and as-cast films of PSHQ*n*, using a General Electric X-ray generator (Model XRD-6) operated at 30 kV and 30 mA (Ni-filtered Cu Kα radiation). The flat-plate diffraction patterns were recorded with a 53.3 mm film-to-specimen distance. The exposure time for each measurement was 4 h. Also conducted were variable-temperature WAXD experiments on as-cast films of PSHQ*n*, using a Rigaku X-ray generator operated at 40 kV and 120 mA. The X-ray beam was monochromatized to Cu Kα with a graphite crystal. The 2θ scanning range employed was 1.3−45° in reflection. A temperature controller with an accuracy of ±1 °C was used, the diffraction patterns being measured at various temperatures ranging from 25 to 280 °C.

A hot-stage (TH-600 type, Linkham Scientific Co.) microscope (Nikon, Model Optiphoto polXTP-11) with a camera, a programmable temperature controller, and photomicrographic attachment were used to take pictures, under cross-polarized light, of films solvent cast on a slide glass.

3. Results and Discussion

3.1. Effect of Flexible Spacer Length on Phase Transitions in PSHQ*n*.

Figure 1 gives DSC traces, obtained during the second heating cycle at a rate of 20 °C/min, for PSHQ*n* having even numbers (4, 6, 8, 10, and 12) of methylene groups. In Figure 1 we observe (1) a glass transition temperature (T_g) and (2), in most cases, two endothermic peaks: (i) a lower temperature endothermic peak, though very weak, representing the solid−mesophase (melting) transition and (ii) a higher temperature endothermic peak representing the mesophase−isotropic transition (isotropization) temperature (also referred to as clearing temperature) (T_{NI}) which increases as the length of methylene groups decreases from 12 to 4. Of particular note in Figure 1 is the appearance of an additional endothermic peak at 243 °C, 16 °C below the T_{NI}, for PSHQ4. According to a previous study of Han et al.,[26] this peak represents the melting temperature of high-temperature melting crystals that were formed, via recrystallization, after the melting of crystals at 185 °C. This indicates that the rate of recrystallizaton is much faster in PSHQ4 than in all other PSHQ*n* having flexible spacers longer than 4. Later in this paper we shall elaborate on the rate of crystallization, observed from variable-temperature X-ray experiment, as affected by the flexible spacer length.

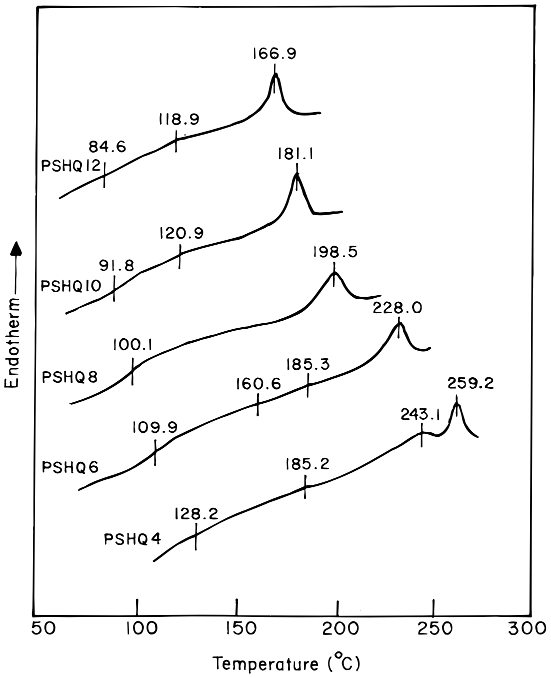

Figure 1. DSC traces during the second heating cycle at a rate of 20 °C/min for as-cast specimens of PSHQ*n* with even numbers of methylene groups of flexible spacer.

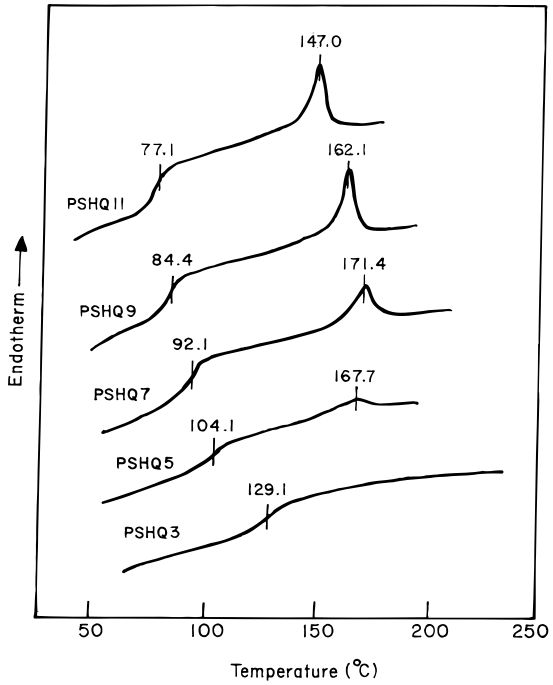

Figure 2. DSC traces during the second heating cycle at a rate of 20 °C/min for as-cast specimens of PSHQ*n* with odd numbers of methylene groups of flexible spacer.

Figure 2 gives DSC traces, obtained during the second heating cycle at a rate of 20 °C/min, for PSHQ*n* having odd numbers (3, 5, 7, 9, and 11) of methylene groups. The following observations are worth noting in Figure 2: (1) this series of PSHQ*n* does not exhibit solid−mesophase transitions (i.e., no melting crystals), (2) PSHQ*n* with flexible spacers of 5, 7, 9, and 11 methylene groups have a broad mesophase region, giving rise to only clearing temperatures which increase as the number of methylene groups decreases, and (3) quite unexpectedly, PSHQ3 undergoes only one transition, a glass transition at ca. 129 °C, over the entire range of temperatures investigated, becoming amorphous above T_g (i.e., it has no liquid crystallinity at all!). Later in this paper we shall elaborate on this by presenting

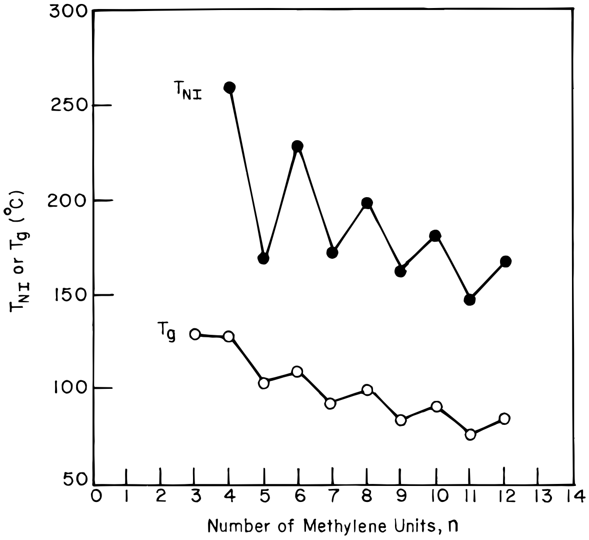

Figure 3. Plots of (●) clearing temperature (T_{NI}) and (○) glass transition temperature versus the number of methylene groups of flexible spacer in PSHQ*n* synthesized in this study.

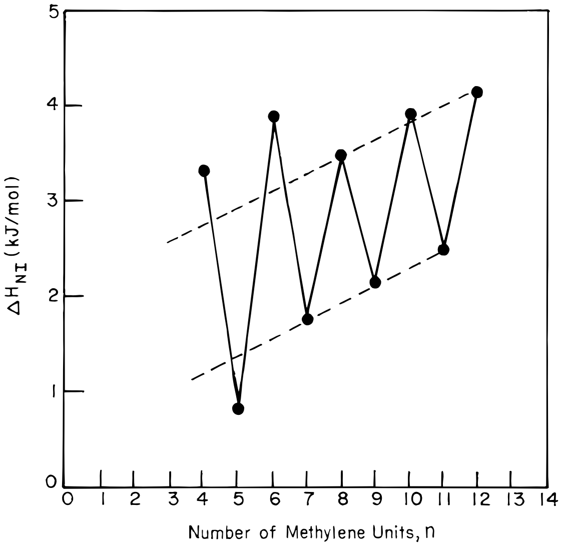

Figure 4. Plots of isotropization enthalpy (ΔH_{NI}) versus the number of methylene groups of flexible spacer in PSHQ*n* synthesized in this study.

further experimental evidence supporting the DSC results. Table 1 gives a summary of thermal transitions of PSHQ*n* synthesized in this study.

Figure 3 describes the dependencies of T_{NI} and T_g on the number of methylene groups of flexible spacer in the ten PSHQ*n* synthesized, showing the well-known odd−even fluctuation in T_{NI}.[1−13] It is of interest to observe in Figure 3 that values of T_g also exhibit odd−even fluctuation, which in the past was rarely observed although many investigators reported odd−even fluctuations in melting temperature.[3−7]

Plots of molar isotropization enthalpy (ΔH_{NI}) versus the number of methylene groups in PSHQ*n* are given in Figure 4. Similar plots were obtained, though not shown here, for molar isotropization entropy (ΔS_{NI}). Previously, using linear main-chain TLCPs (i.e., without pendent side groups), some research groups[5,13,22−24] found that such plots followed linear relationships over the entire range of n values investigated and made the interpretation that the slopes of the linear plots describe the contribution of each methylene unit to the orientational order in the liquid-crystalline phase and the values of ΔH_{NI} (or ΔS_{NI}) at $n = 0$, obtained by extrapolation, describe the contributions from the mesogenic group. However, in Figure 4 we observe linear relationships for values of odd or even n only from 12 to 7, but a deviation from the linear relationship for values of *n* < 7. Another feature in Figure 4, which distinguishes itself from the literature, is that ΔH_{NI} versus n plots (and, also, ΔS_{NI} versus n plots) for even numbers of methylene groups are almost parallel to those for odd numbers of methylene groups, whereas Pardey et al.,[13] for instance, who employed poly(ester imides) which had *no* pendent side groups, reported that ΔH_{NI} versus n plots (and, also, ΔS_{NI} versus n plots) for even and odd numbers of methylene groups merge to a common value at $n = 0$. We speculate that the deviation from the converging linear relationship observed in Figure 4 may be attributable to the presence of the bulky pendent side groups in PSHQ*n*.

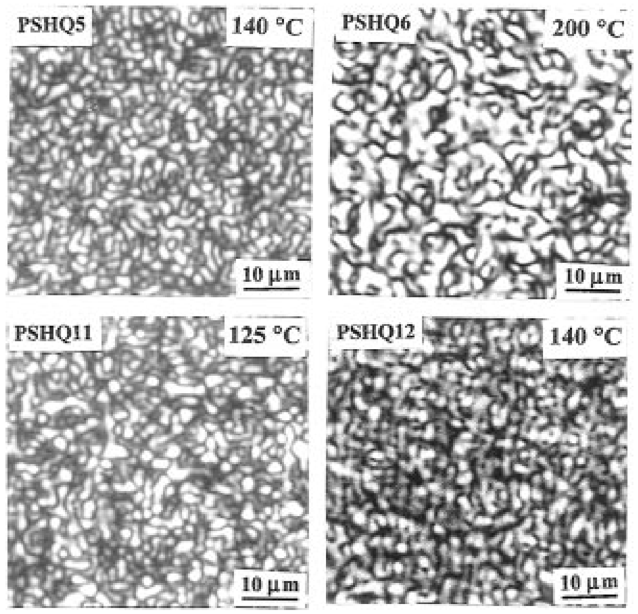

Figure 5. Cross-polarized optical micrographs of PSHQ5, PSHQ6, PSHQ11, and PSHQ12.

It is understood that a linear relationship between ΔH_{NI} and *n* (and, also, between ΔS_{NI} and *n*) indicates that the methylene groups also participate in the ordering process during their transition. In the absence of such a linear relationship in PSHQ*n* with $n < 7$, we tentatively conclude that the bulky pendent side groups in PSHQ*n* play a significant role in the ordering process during their transition. Later in this paper we shall elaborate on this further.

3.2. Mesophase Domain Textures of PSHQ*n* Observed by POM. Figure 5 gives cross-polarized optical micrographs of PSHQ5, PSHQ6, PSHQ11, and PSHQ12. Similar domain textures were observed for the other PSHQ*n*, except for PSHQ3. These micrographs were taken using specimens which were cast from 1,1,2,2-tetrachloroethane solutions and then dried at 70 °C in a vacuum oven. All of the PSHQ samples, regardless of whether they have even or odd numbers of methylene groups of flexible spacer, have a schlieren-textured nematic mesophase. In general, long flexible spacers favor the formation of smectic mesophase while short flexible spacers favor the formation of nematic mesophase in main-chain TLCPs. In the PSHQ*n* synthesized in this study we have not observed such a trend. It should be mentioned that we found *no* domain texture in PSHQ3 over the entire range of temperatures,

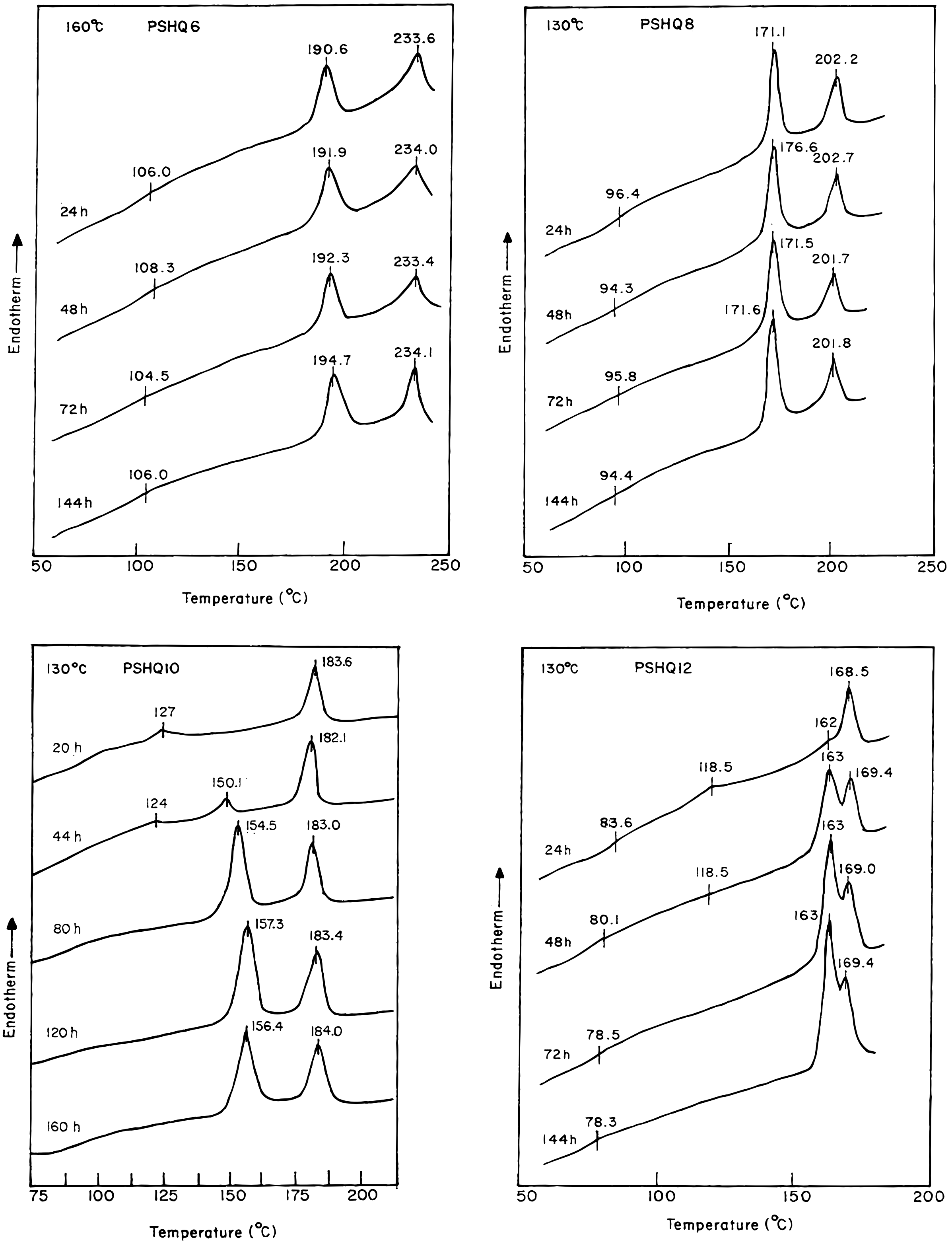

Figure 6. DSC traces during the first heating cycle at a rate of 20 °C/min for as-cast PSHQ*n* specimens with even numbers of methylene groups of flexible spacer after each specimen was heated to an isotropic state and then cooled slowly to a preset temperature in the nematic region followed by annealing there: (i) PSHQ6 annealed at 160 °C for various periods indicated on the plot; (ii) PSHQ8 annealed at 130 °C for various periods indicated on the plot; (iii) PSHQ10 annealed at 130 °C for various periods indicated on the plot; (iv) PSHQ12 annealed at 130 °C for various periods indicated on the plot.

130–180 °C, tested, corroborating the DSC results (see Figure 2) that PSHQ3 indeed is an amorphous polymer.

3.3. Effect of Thermal Treatment on the Phase Transitions and Structural Development in As-Cast PSHQ6, PSHQ8, PSHQ10, and PSHQ12 Specimens. A number of DSC runs were made (not shown here) on as-cast specimens of PSHQ6, PSHQ8, PSHQ10, and PSHQ12, which were annealed for 2 h at various temperatures. We observed that (1) when a specimen was annealed at temperatures below a certain critical value, multiple endothermic peaks appeared, and (2) as the annealing temperature was increased, there was a tendency that an intermediate endothermic peak(s) either disappeared completely or became very small

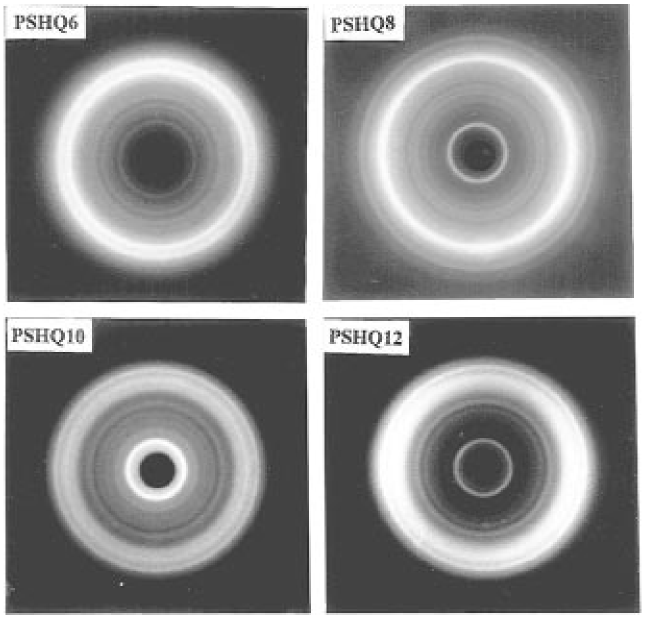

Figure 7. WAXD powder patterns taken at room temperature of PSHQ*n* specimens with even numbers of methylene groups of flexible spacer after each specimen was first heated to an isotropic state and then cooled slowly to a preset temperature in the nematic region followed by annealing there: (i) PSHQ6 annealed at 160 °C for 144 h; (ii) PSHQ8 annealed at 130 °C for 144 h, (iii) PSHQ10 annealed at 130 °C for 144 h; (iv) PSHQ12 annealed at 130 °C for 144 h.

relative to the higher temperature endothermic peak representing T_{NI}.

In order to gain an insight into the nature of the intermediate endothermic peak which appeared in DSC traces, we chose a temperature to further anneal each PSHQ sample for a longer period. From such experiments (not shown here) we observed that initially the intermediate endothermic peak grew with annealing time and then leveled off. According to Han et al.,[26,27] the large intermediate endothermic peak observed represents the melting point (T_{m1}) of high-temperature melting crystals, which were formed via recrystallization during annealing after the melting of solid crystals.

Since we suspected that the as-cast specimens employed in both DSC and WAXD experiments, the results of which are not shown here, could have contained crystals formed by solvent-induced crystallization, we applied thermal treatment to each as-cast PSHQ*n* specimen by first heating to the isotropic region and then cooling slowly down to a predetermined temperature in the nematic region followed by isothermal annealing for a long period. DSC traces of such experiments performed are summarized in Figure 6, from which we observe that all four PSHQ*n* formed considerable amounts of high-temperature melting crystals after annealing for 144 or 160 h. Moreover, Figure 7 gives the WAXD powder patterns taken at room temperature of PSHQ specimens, which also received thermal treatment in the isotropic region followed by isothermal annealing for 144 h in the nematic region. In Figure 7 we observe that all four PSHQ specimens became highly crystalline.

Figure 8 summarizes the variable-temperature X-ray diffraction patterns obtained for unannealed as-cast specimens of PSHQ6, PSHQ8, PSHQ10, and PSHQ12, respectively, during the second heating cycle at a rate of 5 °C/min. It should be mentioned that the shape of the main peak observed during the first cooling cycle, though not shown here, is almost identical to that obtained during the second heating cycle. It is very clear from Figure 8 that the shape of the X-ray diffraction patterns changed little over the entire range of temperatures tested, namely, from 90 to 250 °C for PSHQ6, from 90 to 210 °C for PSHQ8, from 90 to 210 °C for PSHQ10, and from 70 to 190 °C for PSHQ12, although becoming somewhat broader in the isotropic region (see Figure 1 for the transition temperatures of each PSHQ). Notice further in Figure 8 that the peak at large scattering angles is rather broad and there are very weak additional peaks at low scattering angles, suggesting that the ordered structure over the entire anisotropic range of temperatures tested is a one-dimensional liquid-crystalline structure (i.e., nematic mesophase), in complete agreement with the micrographs shown in Figure 5.

3.4. Effect of Thermal Treatment on the Phase Transitions and Structural Development in PSHQ5, PSHQ7, PSHQ9, and PSHQ11. A number of DSC runs were made on as-cast specimens of PSHQ5, PSHQ7, PSHQ9, and PSHQ11, respectively, which were annealed for 2 h at various temperatures. From the DSC traces (not shown here) we observed (i) a small endothermic peak at 102−109 °C for both PSHQ5 and PSHQ7 specimens annealed at 90 °C but not for specimens annealed at higher temperatures, (ii) a very large endothermic peak at 113 °C for PSHQ9 specimens annealed at 90 °C but not for specimens annealed at higher temperatures, and (iii) a large endothermic peak at 116 °C for PSHQ11 specimens annealed at 100 °C and an endothermic peak at 127 °C for specimens annealed at 110 °C, but not for specimens annealed at higher temperatures.

However, when each of the as-cast specimens of PSHQ5, PSHQ7, PSHQ9, and PSHQ11 was annealed at temperatures above its T_g for longer periods, ranging from 24 to 144 h, from the DSC traces (not shown here) we observed (i) only one endothermic peak at ca. 170 °C for PSHQ5 and at ca. 176 °C for PSHQ7, each representing the T_{NI} of the respective polymers, and (ii) a very large lower temperature endothermic peak at 116 °C for PSHQ9 and at 120 °C for PSHQ11, in addition to the higher temperature endothermic peak representing T_{NI}. What was unexpected from those observations is that PSHQ5 and PSHQ7 do not appear to have solid crystals, leading us to conclude that they form a glassy nematic mesophase.

Figure 9 gives DSC traces of PSHQ5, PSHQ7, PSHQ9, and PSHQ11 specimens which were first heated to the isotropic region and then cooled slowly down to the nematic region followed by an isothermal annealing at a preset temperature in the nematic region for various periods ranging from 24 to 144 h. It can be seen in Figure 9 that only one endothermic peak appears, representing T_{NI}, for all four specimens. In other words, all four PSHQ*n* having odd numbers of methylene groups of flexible spacer formed glassy nematic mesophases over the entire range of temperatures tested. This conclusion is supported further by the WAXD powder patterns given in Figure 10, where each specimen was first heated to the isotropic region and then annealed for 144 h at 120 °C for PSHQ5 and PSHQ7 and at 90 °C for PSHQ9 and PSHQ11. From Figures 9 and 10 we can conclude that the crystals that existed in as-cast specimens of PSHQ9 and PSHQ11 originated from solvent-induced crystallization and that these crystals, once melted away during isotropization, do *not*

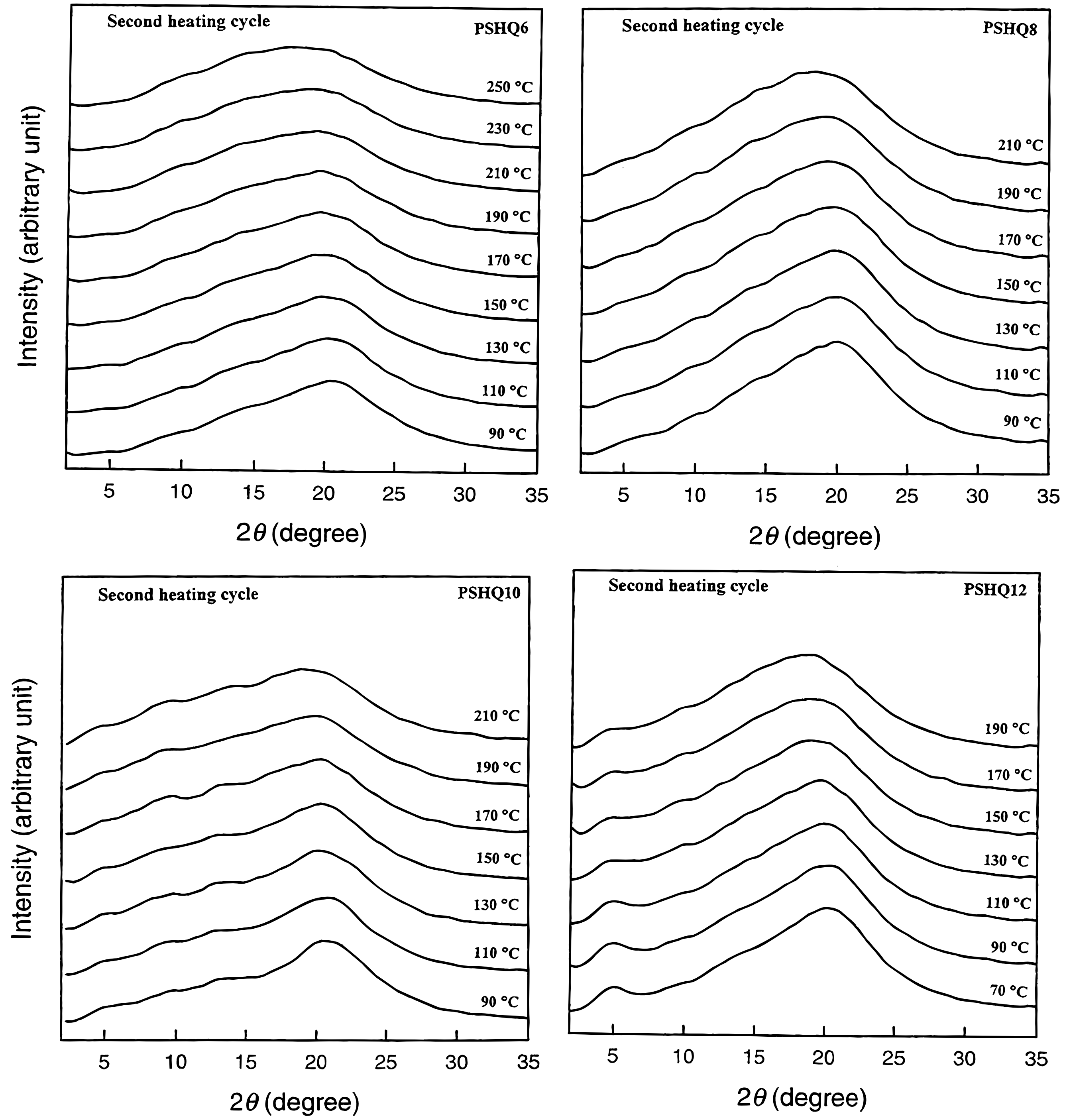

Figure 8. Variation of the X-ray diffraction intensity with scattering angle 2θ for as-cast PSHQn specimens with even numbers of methylene groups of flexible spacer during the second heating cycle at a rate of 5 °C/min.

appear again (i.e., do *not* recrystallize). This conclusion is based on the observations made above (see Figures 6 and 7) that high-temperature melting crystals were formed, via recrystallization, in PSHQ6, PSHQ8, PSHQ10, and PSHQ12 specimens after having received thermal treatment in the isotropic region followed by isothermal annealing for a long period.

Figure 11 summarizes the variable-temperature X-ray diffraction patterns obtained for unannealed as-cast specimens of PSHQ5, PSHQ7, PSHQ9, and PSHQ11, respectively, during the second heating cycle at a rate of 5 °C/min. As for the samples with odd numbers of methylene groups, the shape of the X-ray diffraction patterns changed little over the entire range of temperatures tested, namely, from 90 to 190 °C for PSHQ5, from 90 to 190 °C for PSHQ7, from 70 to 190 °C for PSHQ9, and from 70 to 170 °C for PSHQ11, although becoming somewhat broader in the isotropic region (see Figure 2 for the transition temperatures of each polymer). Notice further in Figure 11 that the peak at large scattering angles is rather broad and there are very weak additional peaks at low scattering angles, suggesting that the ordered structures over the entire anisotropic range of temperatures tested is a one-dimensional liquid-crystalline structure (i.e., nematic mesophase). Comparison of Figure 11 and Figure 8 reveals that the mesophase structure in PSHQ5, PSHQ7, PSHQ9, and PSHQ11 is virtually identical to that in PSHQ6, PSHQ8, PSHQ10, and PSHQ12, confirming again the micrographs given in Figure 5.

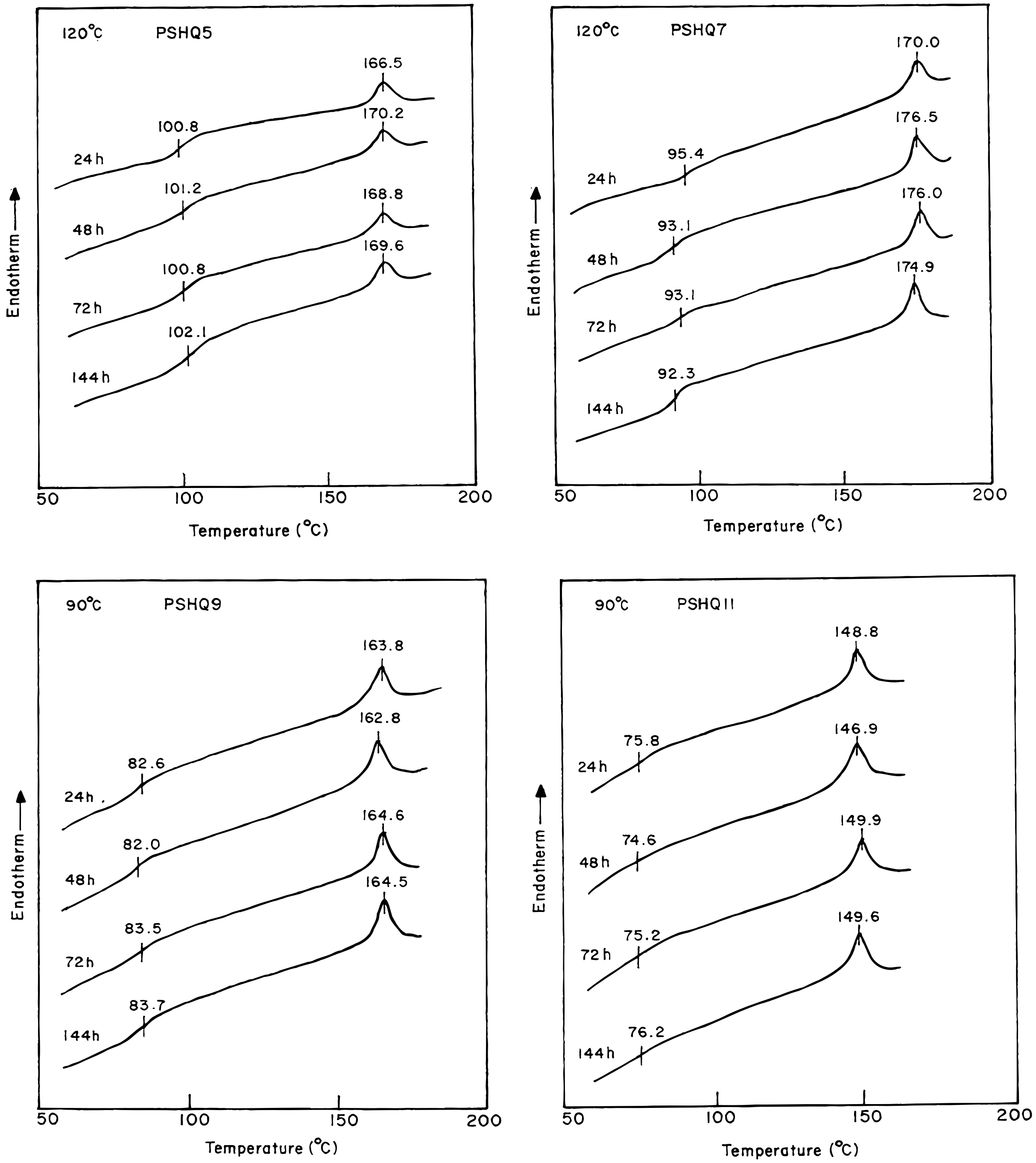

Figure 9. DSC traces during the first heating cycle at a rate of 20 °C/min for as-cast PSHQ*n* specimens with odd numbers of methylene groups of flexible spacer after each specimen was first heated to an isotropic state and then cooled slowly to a preset temperature in the nematic region followed by annealing there: (a) PSHQ5 annealed at 120 °C for various periods indicated on the plot; (b) PSHQ7 annealed at 120 °C for various periods indicated on the plot; (c) PSHQ9 annealed at 90 °C for various periods indicated on the plot; (d) PSHQ11 annealed at 90 °C for various periods indicated on the plot.

3.5. Structural Development in PSHQ3 and PSHQ4. Here we discuss the structural development in PSHQ4 and the lack thereof in PSHQ3, separately from the rest of the PSHQ series synthesized in this study, because (1) PSHQ3 does not form liquid crystals, thus belonging to another class of polymers, and (2) PSHQ4 has the highest rate of crystallization and the highest degree of crystallinity among the ten PSHQ*n* investigated.

Figure 12 compares DSC traces of PSHQ3 with those of PSHQ4 for (i) as-cast specimens annealed for 2 h at various temperatures, as indicated on the plots (upper panel), and (ii) specimens which were first heated to 250 °C for PSHQ3 or to 270 °C for PSHQ4 and then cooled slowly to 130 °C for PSHQ3 and to 190 °C for PSHQ4, followed by an isothermal annealing there for various periods ranging from 24 to 144 h (lower panel). The temperatures, 270 and 190 °C, for PSHQ4 were chosen (see Figure 1) such that the specimen could be heated to the isotropic region and subsequently annealed for recrystallization and perfection. It can be seen in Figure 12 that PSHQ3 exhibits *no* endothermic peak over the entire range of temperatures tested, whereas PSHQ4 exhibits multiple endothermic peaks without or with thermal treatment in the isotropic region.

Notice in the lower right-side panel of Figure 12 that the area of the DSC curve for the 240 °C peak (144 h annealing) is larger than that for the sample annealed

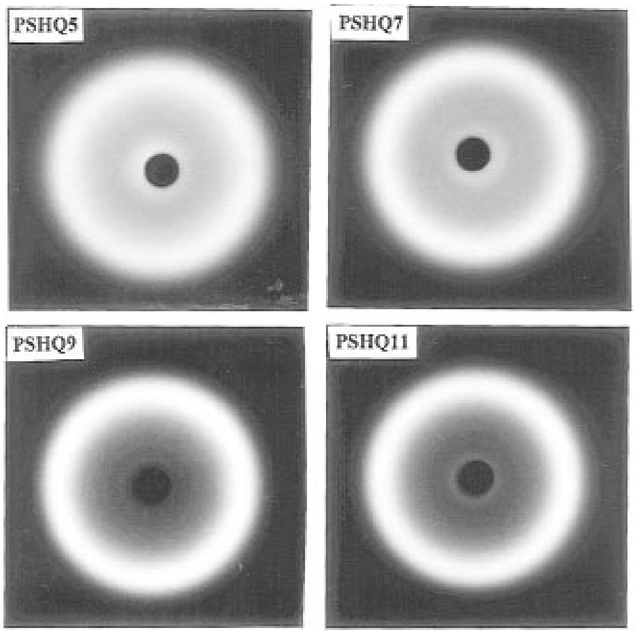

Figure 10. WAXD powder patterns taken at room temperature of PSHQ*n* specimens with odd numbers of methylene groups of flexible spacer after each specimen was first heated to an isotropic state and then cooled slowly to a preset temperature in the nematic region followed by annealing there: (i) PSHQ5 annealed at 120 °C for 144 h; (ii) PSHQ7 annealed at 120 °C for 144 h, (iii) PSHQ9 annealed at 90 °C for 144 h; (iv) PSHQ11 annealed at 90 °C for 144 h.

Table 2. Thermal Transition Properties of High-Temperature Melting Crystals in PSHQ*n* Having Even Numbers of Methylene Groups of the Flexible Spacer

polymer	annealing conditions	T_{m1} (°C)	ΔH_{m1} (kJ/mol)	ΔS_{m1} (J/K mol)
PSHQ4	at 190 °C for 144 h	240.2	11.6	22.5
PSHQ6	at 160 °C for 144 h	194.7	5.1	10.9
PSHQ8	at 130 °C for 144 h	171.6	5.9	13.3
PSHQ10	at 130 °C for 120 h	156.4	5.6	13.0
PSHQ12	at 130 °C for 144 h	163.0	7.9	18.1

for 72 h, suggesting that the crystallization of high-temperature melting crystals continued in PSHQ4 very long periods of temperature at 190 °C. Table 2 gives a summary of the analysis of DSC results, i.e., the change of enthalpy in high-temperature melting crystals, $(\Delta H_{m1})_{iso,ann}$, for PSHQ*n* specimens after being annealed for a long period (120−144 h) in the nematic region. It can be seen in Table 2 that the value of $(\Delta H_1)_{iso,ann}$ is largest (11.56 kJ/mol) for PSHQ4. Further we observed from DSC experiments that the crystallization of other PSHQ*n* (n = 6, 8, 10, and 12) ceased after isothermal annealing in the nematic region for about 48 h. It should be remembered that, in reference to Figure 1, we already have pointed out that the crystallization of PSHQ4 is very fast compared to that of other PSHQ*n* (6, 8, 10, and 12). Earlier, Pardey et al.[13] noted that poly(ester imide)s having odd or even numbers of methylene groups of the flexible spacers became more crystalline as the flexible spacer length increased. Their observation is quite opposite to that presented above for PSHQ*n* with even numbers of methylene groups of the flexible spacers.

Table 3 gives a summary of *d*-spacing of high-temperature melting crystals in PSHQ*n* having even numbers of methylene groups of the flexible spacers. The isothermal annealing conditions employed were the same as given in Table 2. Since our previous study indicated that annealed fiber specimens of PSHQ10 had no strong meridional diffraction at higher 2θ region,[26] we assign the *d*-spacings of 0.44 and 0.40 nm observed in PSHQ10 (see Table 3) to be lateral spacings. Further, since we do not expect that PSHQ*n* would have strong higher order meridional diffractions, such as (006) which may overlap lateral diffractions, we may take the strong diffractions at high 2θ region as lateral spacings of crystals for PSHQ*n*. Comparison of lateral spacings, which describe the interchain distances of the crystal lattices, shows that PSHQ10 and PSHQ12 have a quite compact interchain distance of 0.4 nm, while the interchain distance for PSHQ4, PSHQ6, and PSHQ8, respectively, increases to 0.431−0.471 nm as the number of methylene groups decreases. However, for PSHQ4, another *d*-spacing of 0.378 nm appears which is smaller than the *d*-spacings of PSHQ10 and PSHQ12. We conclude, therefore, that the crystal lattice structures seem to be more regularly ordered due to the increase in the chain linearity and rigidity as the number of methylene groups of the flexible spacers is decreased from 12 to 4. Since there is a maximum in the interchain distances of PSHQ*n* crystals as the n value changes, we speculate that PSHQ6 and PSHQ8 contain a hexagonal crystal lattice while PSHQ4 has an orthorhombic crystal lattice.

WAXD powder patterns of PSHQ3 and PSHQ4 specimens were also taken (not shown here) using the following thermal histories: (i) a PSHQ3 specimen was first heated to 250 °C for 10 min and then cooled slowly down to 130 °C followed by an isothermal annealing there for 144 h, and (ii) a PSHQ4 specimen was first heated to 270 °C for 10 min in the isotropic region and then cooled slowly down to 190 °C in the nematic region followed by an isothermal annealing there for 144 h. From the WAXD powder patterns we concluded that PSHQ3 is amorphous, whereas PSHQ4 has a very high degree of crystallinity. The fact that PSHQ4 has a very high rate of crystallization is manifested further in the variable-temperature X-ray diffraction patterns, given

Table 3. *d*-Spacings (nm) of High-Temperature Melting Crystals in PSHQ*n* Specimens after Receiving Thermal Treatment in the Isotropic Region Followed by an Isothermal Annealing in the Nematic Region[a]

PSHQ4	PSHQ6	PSHQ8	PSHQ10	PSHQ12
1.271 very weak	1.735 weak	1.322 strong	1.354 very strong	1.423 strong
0.871 strong	1.036 medium	0.739 weak	0.970 weak	1.036 weak
0.628 medium	0.712 weak	0.646 weak	0.780 weak	0.684 weak
0.564 medium	0.623 weak	0.592 weak	0.673 weak	0.596 medium
0.471 very strong	0.453 strong	0.431 strong	0.604 weak	0.402 strong
0.422 strong	0.413 strong	0.430 weak	0.584 weak	
0.378 strong		0.357 medium	0.477 weak	
0.346 weak			0.444 medium	
			0.400 strong	
			0.374 weak	

[a] Annealing conditions employed are the same as in Table 2.

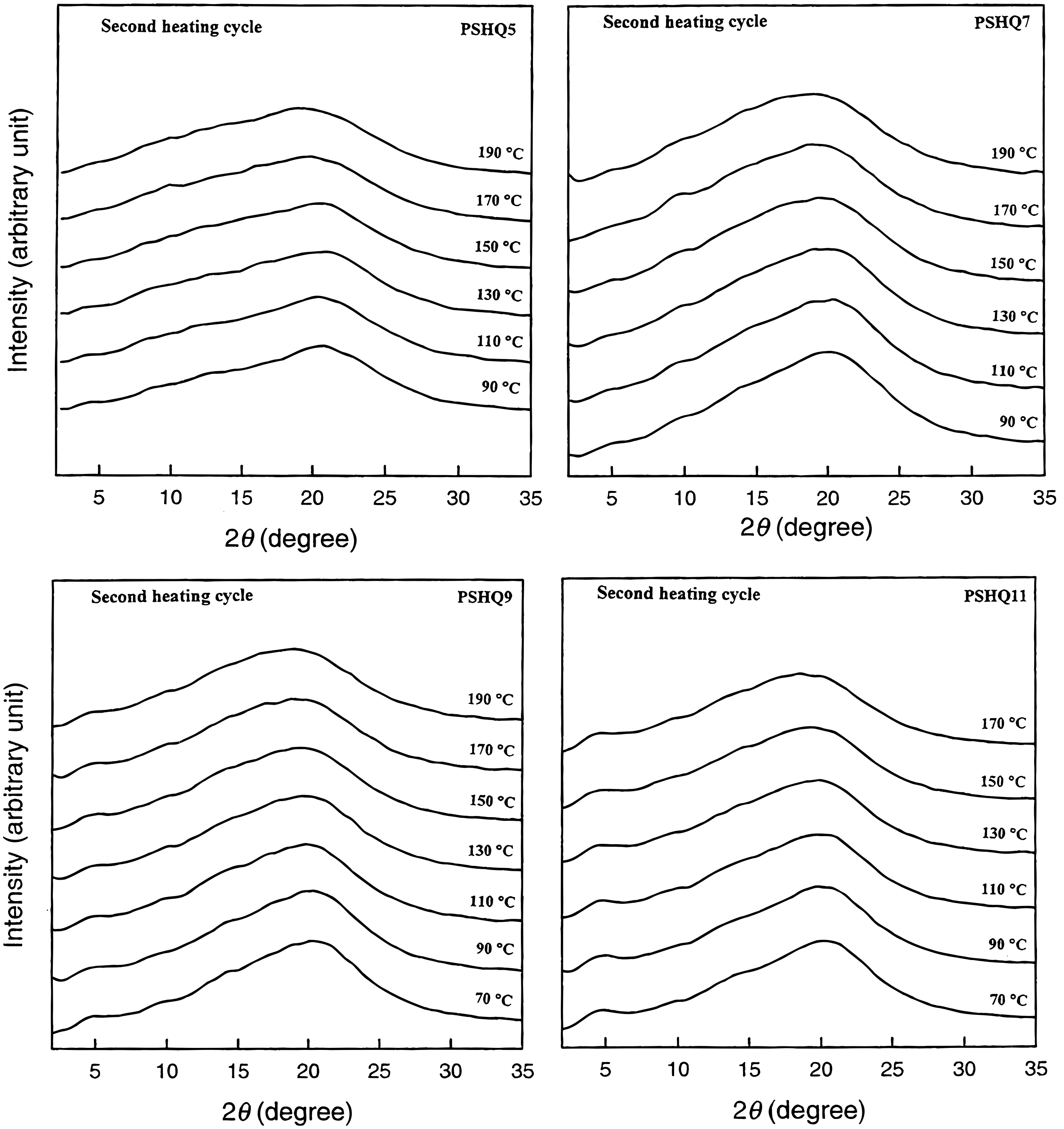

Figure 11. Variation of the X-ray diffraction intensity with scattering angle 2θ for as-cast PSHQ*n* specimens with odd numbers of methylene groups of flexible spacer during the second heating cycle at a rate of 5 °C/min.

in Figure 13, where many reflections at temperatures between 100 and 230 °C are seen. We found that the reflection positions in PSHQ4 in the variable-temperature X-ray diffraction patterns coincide with those in the WAXD powder patterns. Further, comparison of the lower panel of Figure 13 with Figure 8 clearly shows that the rate of crystallization of PSHQ4 is the highest among all PSHQ*n* investigated in this study.

3.6. Odd−Even Effect of Methylene Groups of the Flexible Spacer on the *d*-Spacing of the Chemical Repeating Unit. In order to obtain more detailed information on the structures formed in each of the PSHQ*n* synthesized, WAXD fiber patterns were taken at room temperature of unannealed, melt-drawn fibers of all ten PSHQ*n*. Figure 14 gives, for comparison, WAXD fiber patterns of PSHQ3, PSHQ4, PSHQ7, PSHQ8, PSHQ11, and PSHQ12. With the exception of PSHQ3, (1) there is little difference in X-ray fiber patterns between PSHQ*n* having even numbers of methylene groups or between PSHQ*n* having odd numbers of methylene groups and (2) they all have diffuse lateral spacings, several meridional reflections, and off-axis streaks. As the flexible spacer length increases, the intensity of the lateral streaks becomes stronger, suggesting that a glassy state with axially displaced, nematic chain structures was formed in each fiber sample (especially for $n \geq 8$). From the WAXD fiber patterns taken at room temperature, the lengths of the repeat groups of PSHQ*n* were determined from the spacings of the (002) or (003) reflections and they are

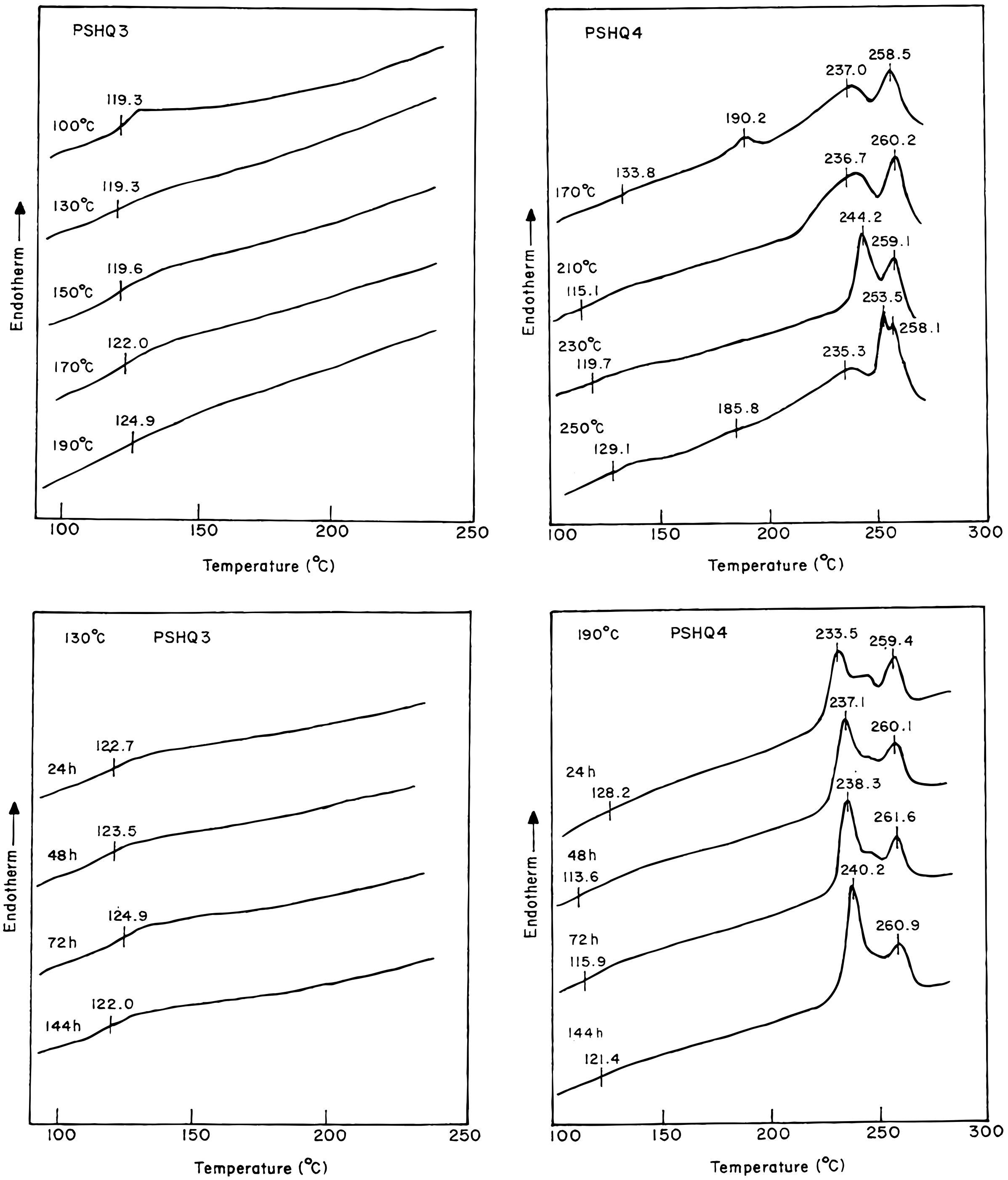

Figure 12. DSC traces for PSHQ3 and PSHQ4 specimens during the first heating cycle at a rate of 20 °C/min, in which the upper panel describes the situation where each as-cast specimen was annealed for 2 h at various temperatures indicated on the plot and the lower panel describes the situation where each specimen was first heated to an isotropic state and then cooled slowly (i) to 130 °C for PSHQ3 and annealed there for 144 h and (ii) to 190 °C for PSHQ4 and annealed there for 144 h.

summarized in Table 4. In addition to the streaks on the first layer lines in all PSHQ*n*, (i) (003) reflections were found in PSHQ*n* having methylene groups greater than 7, and (ii) (002) and (004) reflections were observed in PSHQ4 and PSHQ6. Only a very weak (002) reflection was observed in PSHQ5. For further details of the analysis of WAXD fiber patterns in PSHQ*n*, the readers are referred to our previous paper.[26]

A schematic of the proposed molecular models for PSHQ*n* having different flexible spacer lengths is given in Figure 15, suggesting that the packing of the chain molecules is affected by the existence of the bulky pendent groups. Specifically, for $n < 7$, owing to the short distance between the neighboring mesogenic groups along the chain axis, only one mesogenic group may be placed into the space created by the mesogenic groups of other chain molecules, while for $n > 7$ more spaces between the mesogenic groups along the chain axis are available to accommodate the hindrance caused by the bulky arylsulfonyl side groups. Therefore we speculate that two neighboring mesogenic groups may be allowed to be placed into the space created between the mesogenic groups of other chain molecules. Since this observation was made using unannealed (i.e., quenched) fiber specimens, we speculate that the crystallization would have little effect on this structure.

Figure 16 describes the effect of the flexible spacer length on chemical repeating unit *d*-spacings of PSHQ*n*

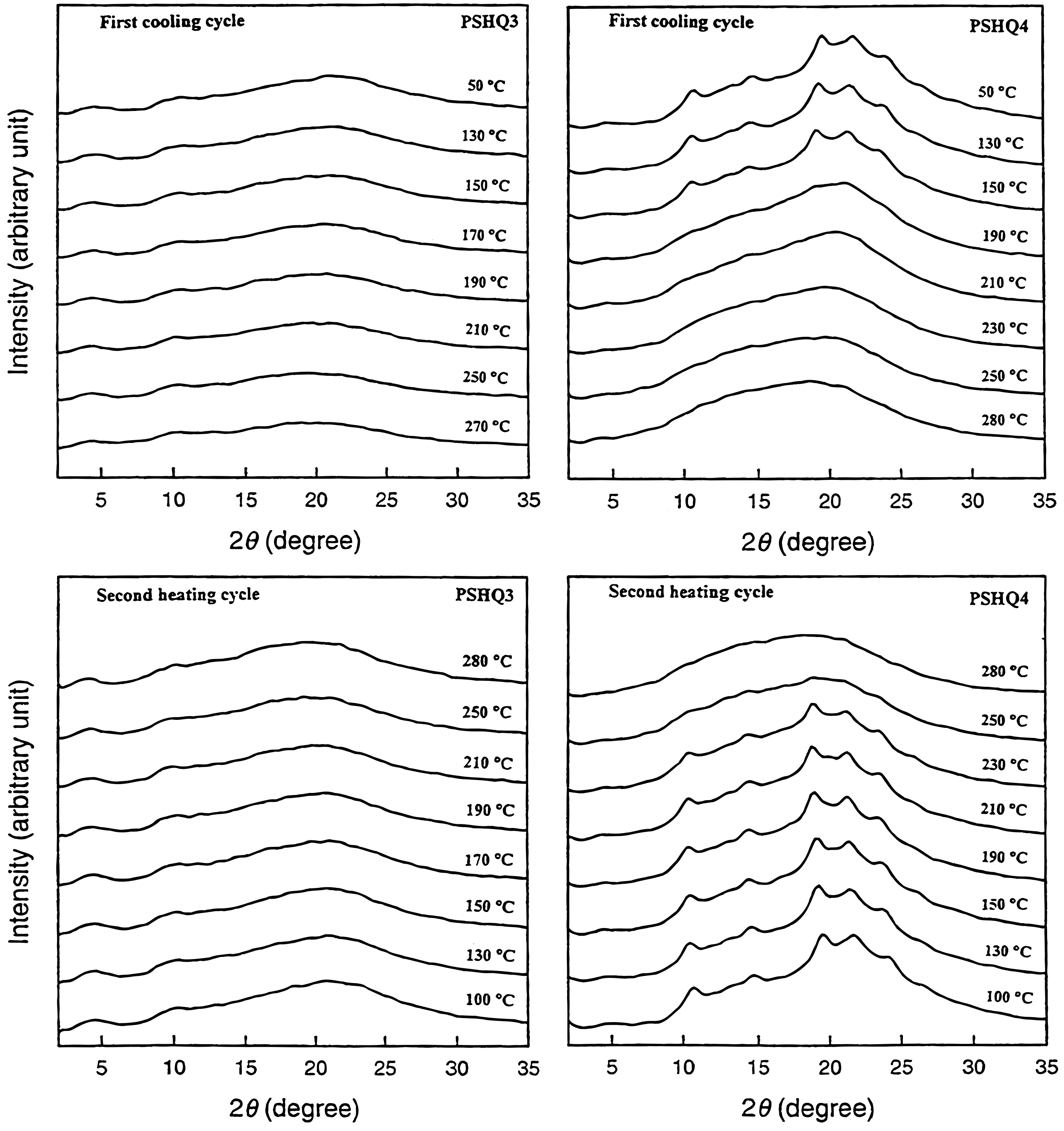

Figure 13. Variation of the X-ray diffraction intensity with scattering angle 2θ for as-cast PSHQ3 and PSHQ4 specimens, in which the upper panel describes the first cooling cycle at a rate of 5 °C/min and the lower panel describes the second heating cycle at a rate of 5 °C/min.

investigated, where the symbol ● denotes values of *d*-spacing obtained from (003) diffraction and the symbol ○ denotes values of *d*-spacing obtained from (002) diffraction. In Figure 16 we observe an odd–even fluctuation of *d*-spacing, similar to that reported in previous studies.[10,11,13,28] We found that PSHQ*n* having odd numbers of methylene groups exhibit distinctly different lateral diffraction, suggesting that the orientational order of chain molecules are lower in PSHQ*n* having odd numbers of methylene groups than in PSHQ*n* having even numbers of methylene groups. This may be due to the conformational restrictions in PSHQ*n* having odd numbers of methylene groups.[29]

From the intercept and slope of the plots given in Figure 16 we obtain the following relationship:

$$\text{(i) } d_{\text{repeat unit, odd}} = 1.660 + 0.1190n_{\text{odd}} \text{ (nm)}$$

$$\text{(ii) } d_{\text{repeat unit, even}} = 1.784 + 0.1148n_{\text{even}} \text{ (nm)}$$

from which we estimate the *d*-spacings of repeat unit in PSHQ*n* having even numbers of methylene groups to be ca. 0.12 nm greater than that in PSHQ*n* having odd numbers of methylene groups. From this information we conclude that axial spacings of mesogenic groups of PSHQ*n* having even numbers of methylene groups are larger than those of PSHQ*n* having odd numbers of methylene groups, suggesting a greater tilting of the mesogenic groups in PSHQ*n* having odd numbers of methylene groups. Due to the existence of off-axis streaks on the first layer line and higher order reflection

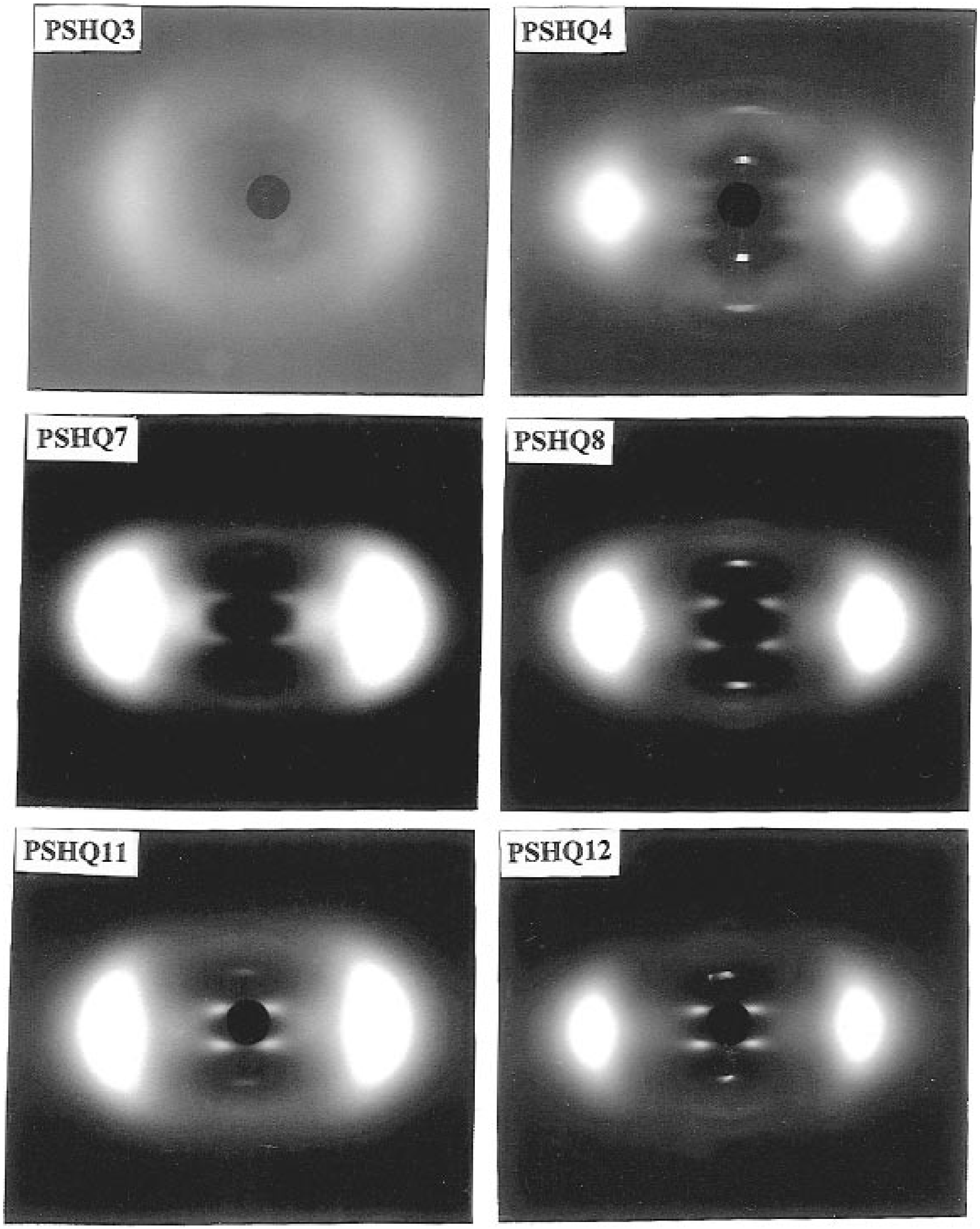

Figure 14. WAXD fiber patterns taken at room temperature of unannealed melt-drawn fibers of PSHQ3, PSHQ4, PSHQ7, PSHQ8, PSHQ11, and PSHQ12.

planes such as (002) or (003) in PSHQ*n*, we assume here that the average alignment of chain molecules, which gives diffraction patterns, is perpendicular to the reflection planes of (002) or (003).

A schematic describing the chain alignment in PSHQ*n* having odd or even numbers of methylene groups of the flexible spacer is given in Figure 17, where the tilting angles of methylene groups of the flexible spacer are determined to be ca. 25° for PSHQ*n* having even numbers of methylene groups and ca. 20° for PSHQ*n* having odd numbers of methylene groups, by assuming a *trans* conformation for the polymethylene groups in PSHQ*n* (0.253 nm for a C−C−C unit). We then conclude that the tilting angle (α) of the mesogenic groups in PSHQ*n* having odd numbers of methylene groups is slightly larger than the tilting angle (β) of the mesogenic groups in PSHQ*n* having even numbers of methylene groups. A precise determination of chain alignment in PSHQ*n* requires conformational analysis, which is beyond the scope of the present study.

4. Concluding Remarks

In this paper we have described the effects of flexible spacer length on phase transitions and the structure of mesophase in a homologous series of thermotropic main-chain liquid-crystalline polyesters, PSHQ*n*, having bulky pendent side groups. Unique observations include the following: (1) there is an odd−even fluctuation of clearing temperature in PSHQ*n*, very similar to the previous findings which employed linear main-chain TLCPs,[1−13] but a deviation from the linear relationship between both the isotropization enthalpy and the isotro-

Table 4. Chemical Repeat Unit *d*-Spacings for Unannealed PSHQ*n* Fibers with Varying Flexible Spacer Lengths

polymer	$2\theta_{(002)}$ (deg)[a]	$2\theta_{(003)}$ (deg)[b]	$d_{(002)}$ (nm)	$d_{(003)}$ (nm)	$d_{(\text{repeat unit})}$ (nm)[c]
PSHQ3					
PSHQ4	7.92		1.12		2.23
PSHQ5	7.87		1.12		2.25
PSHQ6	7.17		1.23		2.47
PSHQ7	7.06[d]	10.53	1.25[d]	0.84	2.52
PSHQ8		9.73		0.91	2.73
PSHQ9		9.73		0.90	2.73
PSHQ10		9.15		0.97	2.90
PSHQ11		8.93		0.99	2.97
PSHQ12		8.40		1.05	3.16

[a] Available for PSHQ*n* having $n \le 7$. [b] Available for PSHQ*n* having $n \ge 7$. [c] *d*-spacings were obtained from $d_{(002)}$ or $d_{(003)}$. [d] This additional (002) reflection is weaker than (003) reflection for PSHQ7 fiber patterns.

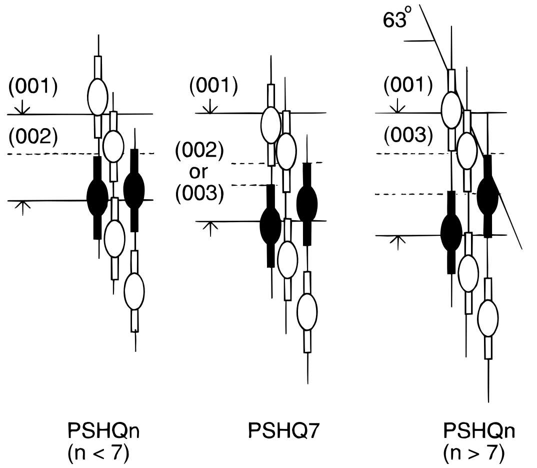

Figure 15. Schematic of the proposed molecular models for PSHQ*n* having different flexible spacer lengths.

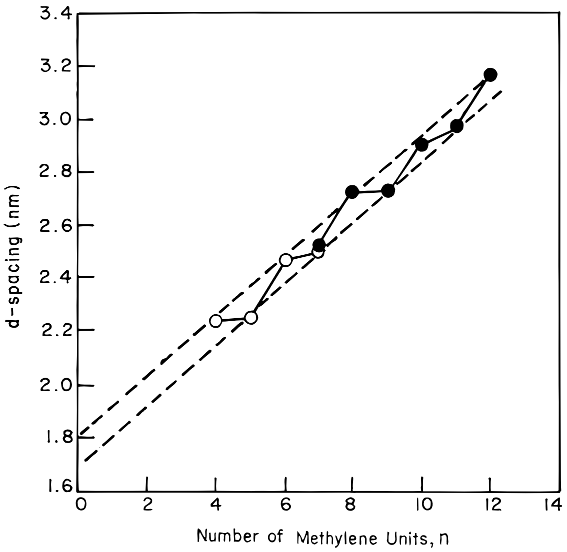

Figure 16. Plots of chemical repeat unit *d*-spacings versus the number of methylene groups of flexible spacers for PSHQ*n*: (○) calculated from the (002) reflection; (●) calculated from the (003) reflection.

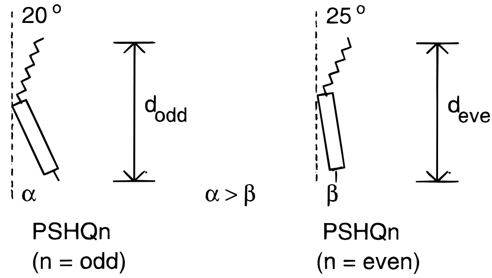

Figure 17. Schematic of the chain alignment in PSHQ*n*.

pization entropy and flexible spacer length, when PSHQ*n* have methylene groups of flexible spacer less than 7; (2) PSHQ*n* having odd numbers (5, 7, 9, and 11) of methylene groups are amorphous polymers, exhibiting only nematic–isotropic transition, and PSHQ*n* having even numbers (4, 6, 8, 10, and 12) of methylene groups are crystalline polymers, exhibiting crystalline–nematic and nematic–isotropic transitions; (3) the rate of crystallization and the degree of crystallinity in PSHQ*n* having even numbers of methylene groups increase as the flexible spacer length decreases, a trend *opposite* to that reported in the literature which dealt with linear main-chain TLCPs; (4) PSHQ3 having three methylene groups of flexible spacer has *no* region of liquid crystallinity, becoming an amorphous polymer with a glass transition temperature of 129 °C. We attribute much of these unexpected observations to the presence of bulky pendent arylsulfonyl side groups in PSHQ*n*. Table 5 gives a summary of the mesophase structures of some main-chain TLCPs with flexible spacers, including those reported in recent literature. At present, there exists no theory predicting the experimental results summarized in Table 5.

Table 5. Mesophase Structures of Some Main-Chain TLCPs with Flexible Spacers

polymer	odd or even *n*	mesophase structure	ref
polyester PB*n*	odd *n* (n =7)	nematic/smectic	8
(enantiotropic)	even *n* ($n = 8$)	smectic	8
polyester BB*n*	odd and even *n*	smectic	9
(enantiotropic)	$n = 5, 6$	smectic	20
(monotropic)	$n = 7, 8, 9$	smectic	20
polyester PSHQ*n*	odd *n* ($n = 3$)	no liquid crystallinity	this study
(enantiotropic)	odd *n* ($n = 5, 7, 9, 11$)	nematic	this study
	even *n* ($n = 4, 6, 8, 10, 12$)	nematic	this study
polyether MBPE*n*	odd *n* ($n = 5, 7, 9, 11$)	nematic/crystalline	22
(monotropic)	even *n*	lack of mesophase transition	22
polyether TPP*n*	odd *n* ($n = 7$)	$I \rightarrow N \rightarrow S_F \rightarrow S_G$	23
(monotropic)	odd *n* ($n = 11$)	$I \rightarrow N \rightarrow S_F \rightarrow S_G \rightarrow S_H$	23
	odd *n* ($n = 15$)	$I \rightarrow S_F \rightarrow S_G \rightarrow S_H$	23
	even *n* ($n = 8$)	$I \rightarrow N \rightarrow S_F \rightarrow S_G \rightarrow S_H$	24
	even *n* ($n = 12$)	$I \rightarrow S_F \rightarrow S_G \rightarrow S_H \rightarrow K_1 \rightarrow K_2$	24
poly(ester imide) PEIM*n* (monotropic)	odd and even *n* ($n = 4-12$)	nematic	11
poly(ester imide) PEIM*n* (monotropic)	odd and even *n* ($n = 4-12$)	smectic	13

On the basis of the observations made above, a number of questions remain to be answered. (1) Why is PSHQ3 an amorphous homopolymer? It has generally been understood that the shorter the length of flexible spacer, the stronger the liquid crystallinity. After all, one inserts flexible spacers into the rigid backbone of a TLCP in order to make it more flexible, thus lowering the clearing temperature. (2) Why do PSHQ*n* having odd numbers of methylene groups form glassy nematic mesophases, whereas PSHQ*n* having even numbers of methylene groups are highly crystalline in the solid state? (3) Why is PSHQ4 so highly crystalline compared to PSHQ6, PSHQ8, PSHQ10, and PSHQ12? (4) Why does the degree of crystallinity appear to decrease with increasing the flexible spacer length in PSHQ*n* having even numbers of methylene groups, whereas the *opposite* trend has been observed in most all other main-chain TLCPs synthesized so far? We believe that many of the answers to these questions are due to the presence of bulky pendent side groups (arylsulfonyl groups) in the PSHQ*n*. It should be noted that all previous studies,[1−13] which reported on odd−even effects of phase transitions in main-chain TLCPs, employed polymers *without* bulky pendent side groups.

In a previous study,[30] we reported differences in phase transition and mesophase structure between PSHQ10 and poly[*p*-phenylene 1,10-decamethylenebis(4-oxybenzoate)] (PHQ10) with chemical structure

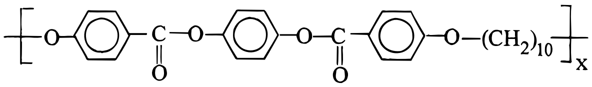

PHQ10 has exactly the same chemical structure as PSHQ10, except that PHQ10 has *no* pendent side groups. PHQ10 undergoes three phase transitions, (i) the solid−smectic transition at 165 °C, (ii) the smectic−nematic transition at ca. 260 °C, and (iii) nematic−isotropic transition at ca. 325 °C. On the other hand, PSHQ10 undergoes only two phase transitions (see Figure 1). The presence of pendent arylsulfonyl side groups in PSHQ10 suppresses the formation of smectic mesophase, giving rise to only a nematic mesophase. In this regard, we speculate that the size of pendent side groups attached to the main chain of a TLCP would play a significant role in controlling not only its phase transitions but also its mesophase structures. This is a subject worth pursuing in future research.

Using the rotational isomeric state (RIS) model, Abe[31] performed conformational analyses of linear main-chain TLCPs having flexible spacers with repeat groups, $-[\mathrm{X}-\mathrm{O}-\mathrm{CO}(\mathrm{CH_2})_n\mathrm{CO}-\mathrm{O}]-$ and $-[\mathrm{X}-\mathrm{O}-\mathrm{O}(\mathrm{CH_2})_n\mathrm{O}-\mathrm{CO}]-$, where X denotes rigid cores of the polymer chains. He concluded that only polymer chains having even numbers of methylene groups conform to the concept of an ordinary nematic ordering, while alignment of rigid cores along one preferred domain axis, due to configurational restrictions imposed by the intramolecular correlation, would be improbable in polymer chains having odd numbers of methylene groups. This suggests that polymers having odd numbers of methylene groups should have mesophases markedly different from regular nematic ordering. He concluded further that for linear main-chain TLCPs with odd numbers of flexible spacers, a simple nematic ordering would be inconsistent with the requirement imposed by conformations of flexible segments. Abe's RIS analysis indicates further that the smectic layers are constructed of highly extended chains and that there is a rather remarkable difference in the arrangement of mesophases of polyesters having odd or even numbers of flexible spacers. In the polymer having even numbers of flexible spacer, the mesogenic groups are approximately parallel to the chain axis, while in polyesters having odd numbers of flexible spacer the mesogenic groups are tilted by about 25−45° to the chain axis, their tilt directions being opposite between the mesogenic groups that are next to each other along the polymer chain. The smectic structure is strongly affected by the conformational constraint of a flexible spacer. Abe concluded that only a nearly parallel orientation of the successive mesogenic groups (with the angle of 0−30 °) is allowed in polymers having even numbers of flexible spacer, while in polymers having odd numbers of flexible spacer two successive mesogens are allowed at an angle in the range of 50−90°.

Yoon and Bruckner[32] also conducted conformational analysis, using the RIS model, for linear main-chain TLCPs comprising rigid groups connected by methylene groups of flexible spacers: (1) Polymer I in which methylene groups are attached by an −O− linkage to a linear rigid group (LR), LR−O−methylene groups, (2) Polymer II having LR−O(O═)C−methylene groups, and (3) Polymer III where the ester unit connection is reversed to LR−C(═O)O−methylene groups. Their analysis concludes that not only is the odd−even effect important, but also the specific groups (or atoms) connected at the ends of methylene groups of flexible spacer. The conclusions in that paper are not as explicit as those in Abe's paper[31] insofar as odd−even effects are concerned.

However, in the present study we observed, with the exception of PSHQ3, only the nematic mesophase in all PSHQ*n* having either odd or even numbers of methylene groups of flexible spacer, which deviates from Abe's prediction.[31] The observed difference between our experimental results and Abe's prediction appears to lie in the fact that the PSHQ*n* employed in our study have bulky pendent side groups, while Abe's theory is based on linear chains, although there is some experimental evidence[8] showing that nematic phases have also been observed for linear TLCPs having odd numbers of flexible spacers. In other words, the pendent bulky arylsulfonyl groups attached to the main chains (rigid cores) of PSHQ*n* appear to have suppressed the molecular packing in the polymer. Readers should be reminded of our previous study,[30] reporting that PHQ10, which has *no* pendent side groups on the main chain and has otherwise the identical chemical structure to PSHQ10, gives rise to a smectic mesophase at temperatures below 260 °C and a nematic mesophase at temperatures above 260 °C until reaching an isotropization temperature, 325 °C. We thus tentatively conclude that the bulky pendent arylsulfonyl side groups attached to the main chain of PSHQ*n* played the decisive role in giving rise to some of the unexpected observations made in this study.

It is worthwhile pursuing (1) more experiments to determine the roles of pendent side groups on phase transitions and the structure of mesophase in main-chain TLCP by varying the size of pendent side groups and (2) conformational analysis of main-chain TLCPs having pendent side groups. Such analyses, when completed successfully, will help the design of new liquid-crystalline polymers.

Acknowledgment. We acknowledge that this study was supported in part by the National Science Foundation under Grant CTS-9320351.

References and Notes

(1) Roviello, A.; Sirigu, A. *Eur. Polym. J.* **1979**, *15*, 61, 423.
(2) Strzelecki, L.; van Luyen, D. *Eur. Polym. J.* **1980**, *16*, 299.
(3) Griffin, A. C.; Havens, S. J. *J. Polym. Sci., Polym. Phys. Ed.* **1981**, *19*, 951.
(4) Antoun, S.; Lenz, R. W.; Jin, J.-I. *J. Polym. Sci., Polym. Phys. Ed.* **1981**, *19*, 1901.
(5) Blumstein, A.; Thomas, O. *Macromolecules* **1982**, *15*, 1264.
(6) Ober, C. K.; Jin, J.-I.; Lenz, R. W. *Polym. J.* **1982**, *14*, 9.
(7) Roviello, A.; Sirigu, A. *Makromol. Chem.* **1982**, *183*, 895.
(8) Krigbaum, W. R.; Watanabe, J.; Ishikawa, T. *Macromolecules* **1983**, *16*, 1271.
(9) Watanabe, J.; Hayashi, M. *Macromolecules* **1988**, *21*, 278.
(10) Kricheldorf, H. R.; Pakull, R. *Macromolecules* **1988**, *21*, 551.
(11) De Abajo, J.; De la Campa, J. G.; Kricheldorf, H. R.; Schwarz, G. *Makromol. Chem.* **1990**, *191*, 537.
(12) Percec, V.; Yourd, R. *Macromolecules* **1989**, *22*, 3229.
(13) Pardey, R.; Shen, D.; Gabori, P. A.; Harris, F. W.; Cheng, S. Z. D.; Adduci, J.; Facinelli, J. V.; Lenz, R. W. *Macromolecules* **1993**, *26*, 3687.
(14) Zhou, Q.-F.; Lenz, R. W. *J. Polym. Sci., Polym. Chem. Ed.* **1983**, *21*, 3313.
(15) Furukawa, A.; Lenz, R. W. *Macromol. Chem., Macromol. Symp.* **1986**, *2*, 3.
(16) Bhowmik, O. K.; Garay, P. O.; Lenz, R. W. *Makromol. Chem.* **1992**, *192*, 415.
(17) Ober, C. K.; Jin, J.-I.; Zhou, Q.; Lenz, R. W. *Adv. Polym. Sci.* **1984**, *59*, 103 and references therein.
(18) Sirigu, A. In *Liquid Crystallinity in Polymers*; Cifferi, A., Ed.; VCH Publishers: New York, 1991; Chapter 7 and references therein.
(19) Percec, V.; Tomazos, D. In *Comprehensive Polymer Science*; Allen, G., Aggarwal, S. L., Rosso, S., Eds.; Pergamon: Oxford, U.K., 1992; First Supplement, pp 300−356.
(20) Watanabe, J.; Hayashi, M. *Macromolecules* **1989**, *21*, 4083.
(21) Pardey, R.; Zhang, A.; Gabori, P. A.; Harris, F. W.; Cheng, S. Z. D.; Adduci, J.; Facinelli, J. V.; Lenz, R. W. *Macromolecules* **1992**, *25*, 5060.
(22) Yandrasits, M. A.; Cheng, S. Z. D.; Zhang, A.; Cheng, J.; Wunderlich, B.; Percec, V. *Macromolecules* **1992**, *25*, 2112.
(23) Yoon, Y.; Zhang, A.; Ho, R.-M.; Cheng, S. Z. D.; Percec, V.; Chu, P. *Macromolecules* **1996**, *29*, 294.
(24) Yoon, Y.; Ho, R.-M.; Moon, B.; Kim, D.; McCreight, K. W.; Li, F.; Harris, F. W.; Cheng, S. Z. D.; Percec, V.; Chu, P. *Macromolecules* **1996**, *29*, 3421.
(25) Kim, S. S.; Han, C. D. *Polymer* **1994**, *35*, 93.
(26) Han, C. D.; Chang, S.; Kim, S. S. *Macromolecules* **1994**, *27*, 7699.
(27) Kim, S. S.; Han, C. D. *Macromolecules* **1993**, *26*, 3176.
(28) Kricheldorf, H. R.; Schwarz, G.; De Abajo, J.; De la Campa, J. G. *Polymer* **1991**, *32*, 942.
(29) Blumstein, A.; Thomas, J.; Asrar, J.; Makris, P.; Clough, S. B.; Blumstien, J. *J. Polym. Sci., Polym. Lett. Ed.* **1984**, *22*, 13.
(30) Chang, S.; Han, C. D. *Macromolecules* **1996**, *29*, 2103.
(31) Abe, A. *Macromolecules* **1984**, *17*, 2280.
(32) Yoon, D. Y.; Bruckner, S. *Macromolecules* **1985**, *18*, 651.

MA961730N